JOURNAL OF GUIDANCE, CONTROL, AND DYNAMICS
Vol. 23, No. 2, March–April 2000

Fuel Optimization for Constrained Rotation of Spacecraft Formations

Randal W. Beard* and Timothy W. McLain†
Brigham Young University, Provo, Utah 84602
and
Fred Y. Hadaegh‡
Jet Propulsion Laboratory, California Institute of Technology, Pasadena, California 91101

The problem of reorienting a constellation of spacecraft such that the fuel distributed across the constellation is both conserved and expended uniformly is considered. Results are derived for constellations with an arbitrary number of spacecraft, assuming that the constellation is in free space, that the spacecraft mass is time invariant, and that the thrusters can produce thrust in any direction. An open-loop control algorithm is derived by minimizing a cost function that trades off total fuel minimization and fuel equalization. The associated optimization problem is shown to be amenable to standard algorithms. Simulation results using a four-spacecraft constellation are given.

Introduction

MULTIPLE spacecraft formation flying is emerging as an enabling technology for a number of planned NASA missions. An example is the proposed separated spacecraft interferometry missions.[1] (Also access "The New Millennium Separated Spacecraft Interferometer," by K. Lau, M. Colavita, and M. Shao at http://www.spacebase.jpl.nasagov.) Because the life expectancy of a satellite is limited by its fuel, fuel optimization is critically important to formation control algorithms. For various applications of spacecraft formation flying, including interferometry, the formation is required to assume several orientations. In this paper we will consider the problem of rotating a formation from one orientation to another. A key observation is that the inertial point about which the formation rotates determines the amount of fuel consumed by each spacecraft. For example, if the formation rotates about a single spacecraft, then that spacecraft will not consume fuel, while the other spacecraft consume disproportionately large amounts of fuel. The objective of this paper is to evaluate strategies for determining a fuel-optimal point of rotation given the current and desired constellation configurations and rotation angles. In evaluating these strategies, two quantities are of primary interest: the total fuel used by the spacecraft in the constellation and the distribution of fuel usage among the spacecraft in the constellation. Not only is it desirable to minimize the total combined fuel expended by the formation during a maneuver, it is perhaps even more desirable to ensure that no spacecraft is starved of fuel, that is, it is desirable that all of the spacecraft run out of fuel simultaneously. The reason that it is important to avoid fuel starvation for interferometry missions is because when one spacecraft runs out of fuel the mission must be terminated, even though the remaining spacecraft still have fuel. It turns out that fuel minimization and equalization are competing objectives. The contribution of this paper is to derive open-loop control strategies that explicitly tradeoff these two objectives.

Central to these control strategies is the determination of the point of rotation for the constellation. This paper will explore how to pick a point of rotation such that the fuel distribution at the end of the maneuver is equalized and the total fuel expended by the constellation is as small as possible. This is done by formulating a cost function containing two terms. The first term penalizes the fuel expended during a maneuver. The second term is motivated by the entropy function from information theory that has the property that it is maximized by a uniform probability mass function,[2] thereby penalizing an unequal fuel distribution at the end of the maneuver. The point of rotation for the constellation is obtained by optimizing this cost function. Once the point of rotation is determined, it is fixed for the duration of the constellation rotation and cannot adapt to reflect fuel expenditure that may be different than what was anticipated.

Wang and Hadaegh developed formation flying strategies for tightly controlled satellite constellations using nearest neighbor tracking laws to maintain relative position and attitude between spacecraft.[3] Their approach is extended in Ref. 4 to the problem of continuous rotational slews.

The application of space-based formation flying to interferometry is discussed in Ref. 1. DeCou[5] studies passive formation control for geocentric orbits in the context of interferometry. McInnes[6] uses Lyapunov control functions to maintain a constellation of satellites in a ring formation. Ulybyshev[7] uses a linear quadratic (LQ) regulator approach for relative formation keeping. Formation initialization has been studied in Ref. 8.

An approach related to Ref. 3 is reported in Refs. 9 and 10. The basic idea is to treat the spacecraft constellation as a system of bodies that are fixed relative to each other and then to control the system as a whole.

Preliminary results were originally reported in Ref. 11, where fuel optimization was performed in two dimensions. Similar results are reported in Ref. 12, where the spacecraft are not required to maintain relative positioning throughout the maneuver.

The remainder of this paper is organized as follows. First, our notation is defined, and the basic assumptions made throughout the paper are stated. Second, the cost function is defined, and the basic open-loop control algorithm is derived. Third, the cost function is analyzed and an optimization algorithm is discussed. Fourth, the simulation results using a constellation with four spacecraft are discussed. Finally, the last section gives our conclusions.

Definitions and Assumptions

This section establishes the notation and assumptions that will be used throughout the paper. Assuming that there are N spacecraft in the constellation, define $N + 2$ coordinate frames as follows. Let $\mathcal{C}_0$ be the inertial coordinate frame with orthonormal basis vectors $\{\boldsymbol{i}_0, \boldsymbol{j}_0, \boldsymbol{k}_0\}$. Let $\mathcal{C}_R$ be a coordinate frame designated as the rotation frame, with orthonormal basis vectors $\{\boldsymbol{i}_R, \boldsymbol{j}_R, \boldsymbol{k}_R\}$. The frame $\mathcal{C}_R$ is used to specify the point of rotation of the constellation. Each

Received 4 January 1999; revision received 6 July 1999; accepted for publication 30 July 1999.

*Assistant Professor, Department of Electrical and Computer Engineering. Member AIAA.

†Assistant Professor, Department of Mechanical Engineering. Member AIAA.

‡Senior Research Scientist and Technical Supervisor, Automation and Control Section. Associate Fellow AIAA.

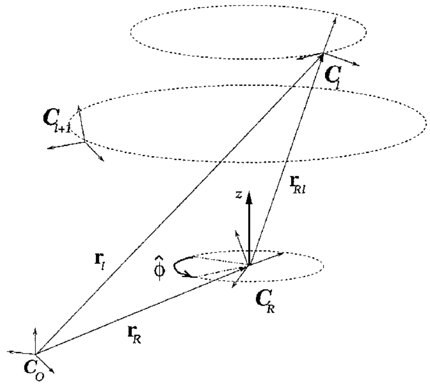

Fig. 1 Problem geometry.

of the N spacecraft is associated with a coordinate frame $\mathcal{C}_\ell$ with associated orthonormal bases $\{\boldsymbol{i}_\ell, \boldsymbol{j}_\ell, \boldsymbol{k}_\ell\}$.

Let $\boldsymbol{r}_\ell$, and $\boldsymbol{r}_R$ be the position vectors of coordinate frames $\mathcal{C}_\ell$, and $\mathcal{C}_R$, respectively, in the inertial frame. Also let $\boldsymbol{r}_{R\ell}$ be defined as the vectors from $\mathcal{C}_R$ to $\mathcal{C}_\ell$. To maintain the constellation formation throughout a rotation maneuver, it is desired that $\boldsymbol{r}_{R\ell}$ remain constant with respect to the rotation frame $\mathcal{C}_R$. The geometry is shown in Fig. 1.

Define M_ℓ to be the mass of the ℓth spacecraft and $f_\ell(t)$ to be the fuel mass contained on the ℓth spacecraft at time t. Furthermore, assume each spacecraft is equipped with an orthogonal set of thrusters capable of producing thrust $\boldsymbol{T}_\ell$ in any direction. The dynamics for the ℓth spacecraft are modeled by the following equations:

$$M_\ell \ddot{\boldsymbol{r}}_\ell = \begin{cases} \boldsymbol{T}_\ell, & f_\ell(t) > 0 \\ 0, & \text{otherwise} \end{cases}$$

$$\dot{f}_\ell = \begin{cases} -\gamma(|T_{a\ell}| + |T_{r\ell}| + |T_{t\ell}|), & f_\ell(t) > 0 \\ 0, & \text{otherwise} \end{cases} \tag{1}$$

where γ is a proportionality constant and $T_{a\ell}$, $T_{r\ell}$, and $T_{t\ell}$ are the axial, radial, and transverse components of $\boldsymbol{T}_\ell$ expressed in the $\mathcal{C}_\ell$ coordinate frame.

The control objective is to rotate the entire constellation through an angle $\hat{\phi}$ about a unit vector z that is referenced to the coordinate frame $\mathcal{C}_R$. This rotation can be specified by a unit quaternion $\boldsymbol{q} = [z^T \sin(\hat{\phi}/2), \cos(\hat{\phi}/2)]^T$. Given a rotation quaternion $\boldsymbol{q}$, the quantities z and $\hat{\phi}$ can be found by the inverse quaternion formulas given in Ref. 13.

The major assumptions made throughout the paper are as follows. 1) The constellation is in free space. 2) The thrust magnitude of the thrusters for an individual spacecraft is finite, but collectively the thrusters can produce force in any direction. 3) Each spacecraft is a rigid body with mass that is time invariant. 4) Rotations of the spacecraft are carried out using means other than thrusters, for example, momentum wheels; therefore, rotational motion is not considered when calculating fuel usage. 5) The position $\boldsymbol{r}_\ell$ of each spacecraft can be determined with respect to the coordinate frame $\mathcal{C}_O$. 6) The thrust magnitude is allowed to range continuously between the saturation limits of the thruster.

Note that these assumptions imply perfect navigation information and perfect thruster performance. Robustness of the derived methods with respect to imperfect navigation information and thrusters has not been studied.

If any of these assumptions are relaxed, the results of this paper will need to be modified. For example, if the constellation is not in free space, then orbital dynamics will affect the fuel consumption. If certain thrust directions cannot be produced, then a sequence of maneuvers may be required to accomplish a rotation, thereby requiring a different fuel analysis. If the mass of the fuel is on the order of the mass of the spacecraft, then the analysis would need to be modified to use the rocket equation. Similarly, rotational dynamics would add an additional level of complexity. Addressing the last two assumptions is necessary to accomplish fixed-formation maneuvers in general.

Static Rotations

This section derives an algorithm for picking the location of the rotation point, that is, $\boldsymbol{r}_R$, such that, given the initial fuel distribution $\{f_1(t_0), \ldots, f_N(t_0)\}$, the final fuel distribution $\{f_1(t_0 + t_f), \ldots, f_N(t_0 + t_f)\}$ minimizes the following functional:

$$J = \min_{r_R} \left\{ \sum_{\ell=1}^{N} [f_\ell(t_0) - f_\ell(t_0 + t_f)]^2 + \mu \sum_{\ell=1}^{N} \frac{f_\ell(t_0 + t_f)}{\Sigma_{j=1}^{N} f_j(t_0 + t_f)} \log \frac{f_\ell(t_0 + t_f)}{\Sigma_{j=1}^{N} f_j(t_0 + t_f)} \right\} \tag{2}$$

The first term in this functional represents the total amount of fuel expended by the constellation. The second term is motivated by the negative entropy of a probability distribution (Ref. 2, pp. 12–15), which is minimum for a uniform distribution, that is, the second term will be minimized when $f_i(t_0 + t_f) = f_j(t_0 + t_f)$ for all $i, j \in \{1, \ldots, N\}$.

An alternative to entropy is the function

$$\sum_{i=1}^{N} \sum_{j \neq i}^{N} [f_i(t_0 + t_f) - f_j(t_0 + t_f)]^2 \tag{3}$$

which is also minimized when $f_i(t_0 + t_f) = f_j(t_0 + t_f)$. The use of Eq. (3) gives similar results to those reported in this paper. The entropy term was selected because in simulation studies it equalized the fuel distribution more uniformly.

To minimize Eq. (2), we need to express $f_\ell(t_0 + t_f)$ in terms of $\boldsymbol{r}_R$. For a given $\boldsymbol{r}_R$, we find $f_\ell(t_0 + t_f)$ in two steps: First, determine a constellation rotation trajectory within the thrust capability of each spacecraft in the constellation. Second, calculate the fuel consumed by each spacecraft in following the rotation trajectory. The details of these steps are discussed in the next two sections.

Constellation Rotation Trajectory

Note that the rotational acceleration for the constellation is limited by the linear acceleration capability of each spacecraft and by the distance of each spacecraft from the axis specified by z. Because we are considering the rotation of individual spacecraft about a fixed axis in space, the acceleration of each spacecraft is composed of transverse and radial (centripetal) accelerations with respect to the rotation axis: $\boldsymbol{a}_\ell = \boldsymbol{a}_{t\ell} + \boldsymbol{a}_{r\ell}$, where $\boldsymbol{a}_{t\ell}$ and $\boldsymbol{a}_{r\ell}$ are the transverse and radial accelerations, respectively.

Let $\boldsymbol{d}_\ell$ be the shortest vector between the rotation axis z and the ℓth spacecraft, and define $\phi(t)$ as the constellation rotation angle. The vector $\boldsymbol{d}_\ell$ can be found by using the geometry shown in Fig. 2. The projection of $\boldsymbol{r}_{R\ell}$ onto the z axis is given by $z^T\boldsymbol{r}_{R\ell}$, where z and $\boldsymbol{r}_{R\ell}$ are referenced to the same coordinate frame. Therefore, the shortest vector from the z axis to $\mathcal{C}_\ell$ is

$$\boldsymbol{d}_\ell = \boldsymbol{r}_{R\ell} - (z^T\boldsymbol{r}_{R\ell})z = (I - zz^T)\boldsymbol{r}_{R\ell} \tag{4}$$

where I is the 3×3 identity matrix.

For general rotations, $\|\boldsymbol{a}_{r\ell}\| = \|\boldsymbol{d}_\ell\|\dot{\phi}^2$ and $\|\boldsymbol{a}_{t\ell}\| = \|\boldsymbol{d}_\ell\|\ddot{\phi}$; therefore it can be seen that the magnitude of the acceleration for each spacecraft is proportional to the distance of the spacecraft from the rotation axis:

$$\|\boldsymbol{a}_\ell\| = \|\boldsymbol{d}_\ell\|\sqrt{\ddot{\phi}(t)^2 + \dot{\phi}(t)^4}$$

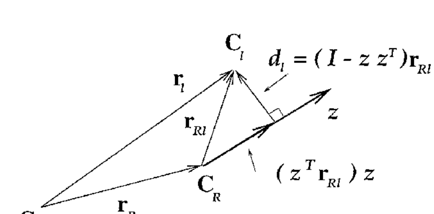

Fig. 2 Distance of the ℓth spacecraft to the z axis.

If we define τ_ℓ as the magnitude of the smallest available maximum thrust in any direction for the ℓth spacecraft (i.e., spacecraft ℓ can produce a thrust of at least τ_ℓ in any specified direction), then the lowest maximum linear acceleration that each spacecraft is capable of is τ_ℓ / M_ℓ:

$$\|\boldsymbol{d}_\ell\|\sqrt{\ddot{\phi}(t)^2 + \dot{\phi}(t)^4} \le \tau_\ell / M_\ell$$

The maximum angular acceleration of the constellation will be maximally constrained by the linear acceleration capability of the spacecraft in the constellation. Specifically, the spacecraft with the largest ratio between the distance from the z axis ($\|\boldsymbol{d}_\ell\|$) and its acceleration capability (τ_ℓ / M_ℓ) will limit the angular acceleration of the entire constellation. Denoting the index of the limiting spacecraft as β gives

$$\beta = \arg \max_{1 \le \ell \le N} (M_\ell / \tau_\ell)\|\boldsymbol{d}_\ell\| \tag{5}$$

The angular motion of the entire constellation, given by $\phi(t)$, must be constrained according to the following relation:

$$\sqrt{\ddot{\phi}(t)^2 + \dot{\phi}(t)^4} \le \tau_\beta / M_\beta \|\boldsymbol{d}_\beta\| \tag{6}$$

By constraining the motion in this manner, the required thrust to track whatever trajectory is specified will never exceed the thrust capabilities of any of the spacecraft. Furthermore, this conservative approach leaves some excess thrust capability for rejecting disturbances or responding to tracking errors.

To estimate the amount of fuel spent by each spacecraft during a constellation rotation, a trajectory for the rotation must be determined. The analysis given here assumes that the constellation is rotated via a trajectory corresponding to a bang-off-bang acceleration profile. This thrust profile is optimal (Ref. 14, pp. 675–710) for a double-integrator plant with actuator saturation. Although linear accelerations during the acceleration and deceleration phases of the trajectory are not constant for each spacecraft (the centripetal component changes with $\dot{\phi}$), the assumption of a bang-off-bang trajectory is a reasonable approach for the constellation rotation problem. The analysis approach taken is not limited to bang-off-bang trajectories. Other trajectories, such as polynomial splines, could be analyzed as well.

Letting $\phi(t)$ be the rotation angle of the constellation about the z axis at time t, where t_0 is the starting time for the rotation, the rotation trajectory for the constellation is given by the following equations

$$\ddot{\phi}(t) = \begin{cases} \alpha, & 0 \le t \le t_w \\ 0, & t_w \le t \le t_f - t_w \\ -\alpha, & t_f - t_w \le t \le t_f \end{cases}$$

$$\dot{\phi}(t) = \begin{cases} \alpha t, & 0 \le t \le t_w \\ \alpha t_w, & t_w \le t \le t_f - t_w \\ \alpha(t_f - t), & t_f - t_w \le t \le t_f \end{cases}$$

$$\phi(t) = \begin{cases} \frac{1}{2}\alpha t^2, & 0 \le t \le t_w \\ \alpha\left[t_w t - t_w^2/2\right], & t_w \le t \le t_f - t_w \\ \alpha\left[t_w(t_f - t_w) - (t_f - t)^2/2\right], & t_f - t_w \le t \le t_f \end{cases} \tag{7}$$

where t_w is the width of the thrust pulse.

Notice that the maximum linear acceleration for each of the spacecraft in the constellation occurs at $t - t_0 = t_w$ when $\ddot{\phi}(t)$ and $\dot{\phi}(t)$ are at their maxima simultaneously: $\ddot{\phi}(t_w + t_0) = \alpha$ and $\dot{\phi}(t_w + t_0) = \alpha t_w$.

With the constellation geometry and trajectory type determined, the next step is to formulate an expression that will allow us to solve for the unknown trajectory parameters (α and t_w) given the constellation parameters ($\|\boldsymbol{d}_\beta\|$, τ_β, and M_β) and the specified trajectory parameters ($\hat{\phi}$ and t_f). This is done by first setting the maximum acceleration of spacecraft β (which is tracking the bang-off-bang rotation trajectory) to the acceleration bound:

$$\|\boldsymbol{d}_\beta\|\sqrt{\alpha^2 + (\alpha t_w)^4} = \tau_\beta / M_\beta \tag{8}$$

Noting that $\hat{\phi} = \phi(t_f + t_0) = \alpha t_w(t_f - t_w)$, we can solve for α to obtain

$$\alpha = \hat{\phi} / t_w(t_f - t_w) \tag{9}$$

By substituting for α in Eq. (8) and manipulating the resulting expression, we find that

$$\frac{\hat{\phi}^2}{c^2(1-c)^2} + \frac{\hat{\phi}^4}{(1-c)^4} = \left(\frac{\tau_\beta t_f^2}{\|\boldsymbol{d}_\beta\| M_\beta}\right)^2 \tag{10}$$

where

$$t_w = c t_f, \qquad 0 < c \le \tfrac{1}{2} \tag{11}$$

Further manipulation yields a sixth-order polynomial in c:

$$\Psi(c) = c^6 - 4c^5 + 6c^4 - 4c^3 - [(\hat{\phi}^4 + \hat{\phi}^2 - K)/K]c^2 + 2(\hat{\phi}^2/K)c - \hat{\phi}^2/K = 0 \tag{12}$$

where $K = (\tau_\beta t_f^2 / \|\boldsymbol{d}_\beta\| M_\beta)^2$. When solving this expression for c, we are interested in the real roots that fall within the range $(0, \frac{1}{2})$ because roots outside this range are physically meaningless. As Fig. 3 shows, solution of Eq. (12) results in four scenarios of interest: 1) no roots between 0 and $\frac{1}{2}$, 2) two identical roots between 0 and $\frac{1}{2}$, 3) two different roots between 0 and $\frac{1}{2}$, and 4) one root between 0 and $\frac{1}{2}$. Case 1 results when the trajectory duration t_f is too short for spacecraft β to accomplish the trajectory given the rotation angle and its acceleration capabilities. Case 2 occurs when the minimum possible trajectory duration that is within the capabilities of spacecraft β is chosen. Case 3 is unusual in that two different values of c are found that result in Eq. (8) being satisfied. However, the smaller value of c gives a more fuel-efficient trajectory and, therefore, is chosen when case 3 occurs. Case 4 occurs when the acceleration capabilities of the spacecraft are not stressed by the selection of t_f.

In selecting the trajectory duration, two specific conditions are of interest: case 2 that results in the minimum possible trajectory duration for the formation and the transition between cases 3 and 4 where one real root is equal to $\frac{1}{2}$. We will consider the latter condition first.

If t_f is chosen to be sufficiently large, case 4 results, and the desired trajectory is well within the capabilities of the spacecraft. The transition between cases 3 and 4 occurs when $t_w = t_f/2$. Letting $t_w = t_f/2$ in Eq. (9) and substituting into the acceleration bound in Eq. (8) yield

$$\left(\frac{\tau_\beta}{M_\beta\|\boldsymbol{d}_\beta\|}\right)^2 = \frac{\hat{\phi}^2}{(t_f/2)^4} + \frac{\hat{\phi}^4}{(t_f/2)^4}$$

Solving for t_f gives

$$t_{f,4} = 2\sqrt{(M_\beta\|\boldsymbol{d}_\beta\|/\tau_\beta)\hat{\phi}\sqrt{1 + \hat{\phi}^2}}$$

When $t_f = t_{f,4}$ the result is case 3 with one of the roots of Eq. (12) being exactly $\frac{1}{2}$ as expected. If $t_f > t_{f,4}$, then there is always a unique solution in the interval $(0, \frac{1}{2})$.

Of greater interest is the minimum possible trajectory duration $t_{f,\min}$ for the spacecraft formation (case 2). For a given constellation of spacecraft (with predetermined capabilities) and a specified rotation angle $\hat{\phi}$, the selection of trajectory duration t_f determines which of the cases results. As can be seen from Fig. 3, case 2 occurs when $\Psi(c) = 0$ and $\mathrm{d}\Psi/\mathrm{d}c = 0$ for the same $c = c_0$:

$$\left.\frac{\mathrm{d}\Psi}{\mathrm{d}c}\right|_{c=c_0} = \Psi(c)|_{c=c_0} = 0$$

where

$$\frac{\mathrm{d}\Psi}{\mathrm{d}c} = 6c^5 - 20c^4 + 24c^3 - 12c^2 - \frac{2(\hat{\phi}^4 + \hat{\phi}^2 - K)}{K}c + 2\frac{\hat{\phi}^2}{K} \tag{13}$$

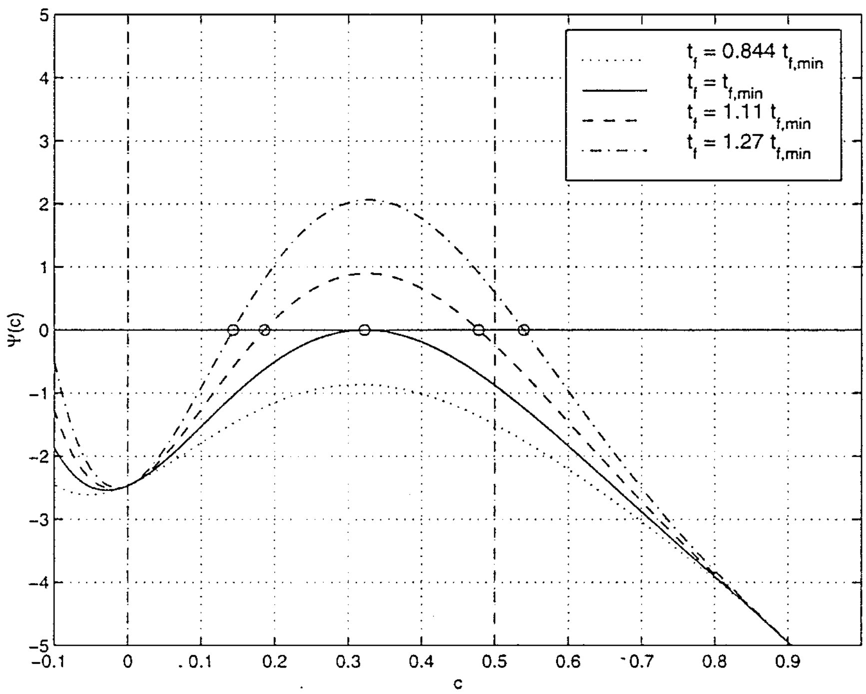

Fig. 3 Roots of $\Psi(c)$.

is determined from Eq. (12). By the equating of the expressions for $\Psi(c)$ and $\mathrm{d}\Psi/\mathrm{d}c$, the following polynomial expression results:

$$c^6 - 10c^5 + 26c^4 - 28c^3 - [(\hat{\phi}^4 + \hat{\phi}^2 - 13K)/K]c^2 + [2(\hat{\phi}^4 + 2\hat{\phi}^2 - K)/K]c - 3\hat{\phi}^2/K = 0 \tag{14}$$

where, in this case, $K = (\tau_\beta t_{f,\min}^2/\|\boldsymbol{d}_\beta\|M_\beta)^2$. This expression can be solved for $c = c_0$ by finding the real root between 0 and $\frac{1}{2}$. Once c_0 is known, the minimum final time $t_{f,\min}$ can be calculated by rewriting Eq. (10) as

$$t_{f,\min} = \left[\left(\frac{\|\boldsymbol{d}_\beta\|M_\beta}{\tau_\beta}\right)^2\left(\frac{\hat{\phi}^2}{c_0^2(1-c_0)^2} + \frac{\hat{\phi}^4}{(1-c_0)^4}\right)\right]^{\frac{1}{4}} \tag{15}$$

Notice that $t_{f,\min}$ is dependent on c_0, that c_0 is dependent on K, and that K is dependent on $t_{f,\min}$. To solve for $t_{f,\min}$, Eqs. (14) and (15) are solved recursively starting with an initial estimate of $t_{f,\min} = t_{f,4}$. Convergence to the solution typically requires only several recursions. From the value of c found from the roots of $\Psi(c)$, values for α and t_w can be calculated from Eqs. (9) and (11), respectively.

In summary, given a specified constellation rotation angle $\hat{\phi}$, trajectory duration $t_f > t_{f,\min}$, thrust capability τ_β, mass M_β, and distance from the rotation axis $\|\boldsymbol{d}_\beta\|$ of the limiting spacecraft, the parameters that complete the characterization of the constellation rotation trajectory can be determined: the switching time t_w and the angular acceleration α.

In this development, we treat the trajectory duration, or alternatively the time required for the formation reorientation to be completed, as a parameter to be selected. Intuitively, the trajectory duration also strongly affects the amount of fuel required to complete the maneuver. If fuel minimization is a high priority, the trajectory duration should be selected as large as possible while still meeting the mission objectives.

Fuel Usage

We must now derive an expression that relates the fuel expended by the ℓth spacecraft to the trajectory of the constellation. The fuel usage for each spacecraft will vary throughout the rotation maneuver and can be calculated for each of the three phases of the trajectory: acceleration, coast, and deceleration.

During the acceleration phase, fuel is expended to accelerate the spacecraft transversely and radially with respect to rotation about the z axis. By drawing on Eq. (1), the fuel expended by spacecraft ℓ during the acceleration phase can be calculated as follows:

$$\begin{aligned} f_\ell(t_w + t_0) - f_\ell(t_0) &= -\gamma\int_{t_0}^{t_w+t_0}(|T_{a\ell}| + |T_{r\ell}| + |T_{t\ell}|)\,\mathrm{d}t \\ &= -\gamma M_\ell\|\boldsymbol{d}_\ell\|\int_{t_0}^{t_w+t_0}\left[\alpha + \alpha^2(t-t_0)^2\right]\mathrm{d}t \\ &= -\gamma M_\ell\|\boldsymbol{d}_\ell\|\alpha\left(t_w + \alpha\frac{t_w^3}{3}\right) \end{aligned}$$

During the coast phase of the trajectory ($t_w < t - t_0 \leq t_f - t_w$), the spacecraft will need to thrust to provide the centripetal acceleration required to track the arc traced out by the constellation. The fuel required to accomplish this is given by

$$\begin{aligned} & f_\ell(t_f - t_w + t_0) - f_\ell(t_w + t_0) \\ &\quad = -\gamma\int_{t_w+t_0}^{t_f-t_w+t_0}(|T_{a\ell}| + |T_{r\ell}| + |T_{t\ell}|)\,\mathrm{d}t \\ &\quad = -\gamma M_\ell\|\boldsymbol{d}_\ell\|\alpha^2 t_w^2\int_{t_w+t_0}^{t_f-t_w+t_0}\mathrm{d}t \\ &\quad = -\gamma M_\ell\|\boldsymbol{d}_\ell\|\alpha^2 t_w^2(t_f - 2t_w) \end{aligned}$$

During the deceleration phase, fuel is expended to bring the spacecraft to a stop and to keep the spacecraft rotating about the z axis. Fuel usage is calculated in a manner similar to the preceding phases:

$$\begin{aligned} & f_\ell(t_f + t_0) - f_\ell(t_f - t_w + t_0) \\ &\quad = -\gamma\int_{t_f-t_w+t_0}^{t_f+t_0}(|T_{a\ell}| + |T_{r\ell}| + |T_{t\ell}|)\,\mathrm{d}t \\ &\quad = -\gamma M_\ell\|\boldsymbol{d}_\ell\|\int_{t_f-t_w+t_0}^{t_f+t_0}(\alpha + \alpha^2(t_f - t + t_0)^2)\,\mathrm{d}t \\ &\quad = -\gamma M_\ell\|\boldsymbol{d}_\ell\|\alpha\left(t_w + \alpha\frac{t_w^3}{3}\right) \end{aligned}$$

The total fuel consumed by the ℓth spacecraft during the rotation of the constellation is given by the sum of the fuel consumed during each of the three phases:

$$f_\ell(t_f + t_0) - f_\ell(t_0) = -\gamma M_\ell \|\boldsymbol{d}_\ell\| \alpha\left(2t_w + \alpha t_w^2 t_f - \tfrac{4}{3}\alpha t_w^3\right) \quad (16)$$

Optimal Point of Rotation

The results of the preceding section can be summarized by the following algorithm for computing the cost function J in Eq. (2).

Algorithm 1: Input $\boldsymbol{r}_R$, $\boldsymbol{q}$, t_f, μ, and $\{\tau_\ell, M_\ell, \boldsymbol{r}_\ell(t_0), f_\ell(t_0)\}_{\ell=1}^N$, and compute the following: 1) z, $\hat{\phi}$; 2) $\boldsymbol{r}_{R\ell}(t_0) = \boldsymbol{r}_\ell(t_0) - \boldsymbol{r}_R$, $\ell = 1, \ldots, N$; 3) $\boldsymbol{d}_\ell(t_0)$, $\ell = 1, \ldots, N$, from Eq. (4); 4) β from Eq. (5); 5) c from Eq. (12); 6) t_w from Eq. (11); 7) α from Eq. (9); and 8) $f_\ell(t_f + t_0)$ from Eq. (16). The output is J from Eq. (2).

It is evident from Eq. (2) and the algorithm just listed that J is a complicated function of $\boldsymbol{r}_R$. It is natural to wonder about the difficulty of optimizing J. The next section contains a mathematical analysis of the cost function and is followed by our recommendations for an algorithm that optimizes J as a function of $\boldsymbol{r}_R$.

Analysis of the Cost Function

The objective of this section is to analyze the nature of J. Figure 4 shows four contour plots of J, projected onto a plane perpendicular to z, as a function of $\boldsymbol{r}_R$ for the parameters listed in Table 1. The ×'s in Fig. 4 represent the location of the spacecraft. The ○ represents the center of inverse fuel mass defined as

$$\boldsymbol{r}_R^{(0)} = \left[\sum_{\ell=1}^{N} \frac{\boldsymbol{r}_\ell(t_0)}{f_\ell(t_0)} \Bigg/ \sum_{j=1}^{N} \frac{1}{f_j(t_0)}\right] \quad (17)$$

Intuitively, $\boldsymbol{r}_R^{(0)}$ will be close to spacecraft that are low on fuel. Figure 4a shows J when the initial fuel is equally distributed among the spacecraft and where fuel equalization is emphasized. Figure 4b shows J when fuel minimization is emphasized. When $\mu = 0$, the initial fuel distribution is not relevant. Figures 4c and 4d are for medium values of μ ($\mu = 100$). Figure 4c shows J when one spacecraft is almost depleted of fuel. In that case, the optimal $\boldsymbol{r}_R$ is located close to the spacecraft that is depleted of fuel. Figure 4d shows J when two spacecraft are almost depleted of fuel. In that case, the optimal $\boldsymbol{r}_R$ is centered between the spacecraft that are low on fuel.

Figure 4 shows cusps in the contour plot J that appear to be aligned along certain lines. These cusps suggest that the gradient of J is discontinuous along these lines. Also, the smoothness of the contours away from these lines suggest that J is continuously differentiable in most of $\mathbb{R}^3$. These observations will be made precise in the following lemmas. The apparent regions come from the partitioning due to Eq. (5). Let $\mathcal{D}_j$ be the region in $\mathbb{R}^3$ that is farther from the jth spacecraft than from any other spacecraft (weighted by M_j/τ_j). These regions can be defined explicitly as follows. Let

$$\mathcal{D}_j = \left\{\boldsymbol{x} \in \mathbb{R}^3 : j = \arg\max_{1 \le \ell \le N} \frac{M_\ell}{\tau_\ell}\|\boldsymbol{d}_\ell - \boldsymbol{x}\|\right\}$$

$$= \bigcap_{i \ne j} \left\{\boldsymbol{x} \in \mathbb{R}^3 : \frac{M_j}{\tau_j}\|\boldsymbol{d}_j - \boldsymbol{x}\| > \frac{M_i}{\tau_i}\|\boldsymbol{d}_i - \boldsymbol{x}\|\right\}$$

Table 1 Parameters for Fig. 4

Parameter	Value
$\boldsymbol{q}$	$[0, 0, \sin(\pi/2), \cos(\pi/2)]^T$
$\boldsymbol{r}_1(t_0)$, m	$(110, 0, 0)^T$
$\boldsymbol{r}_2(t_0)$, m	$(0, 200, 0, 0)^T$
$\boldsymbol{r}_3(t_0)$, m	$(500, -500, 0)^T$
$\boldsymbol{r}_4(t_0)$, m	$(-100, -100, 0)^T$
τ, N	$(700\mu, 700\mu, 700\mu, 700\mu)$
M, kg	(200, 100, 50, 200)
t_f, s	40,000
γ, s/m	0.000088673

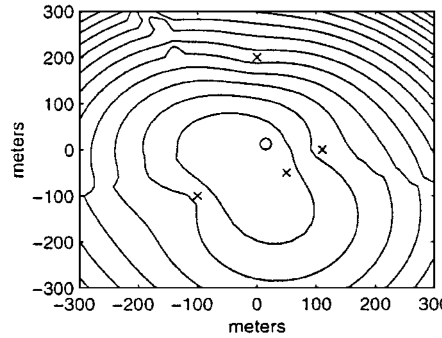

a) $\mu = 10^4$ and $f_\ell(t_0) = [1, 1, 1, 1]$ kg

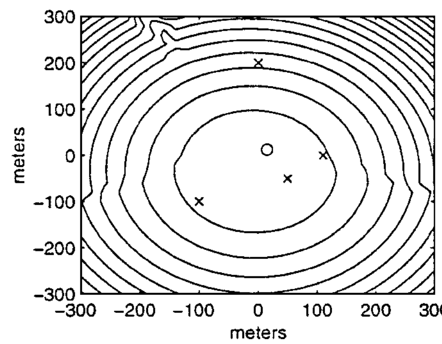

b) $\mu = 0$ and $f_\ell(t_0) = [1, 1, 1, 1]$ kg

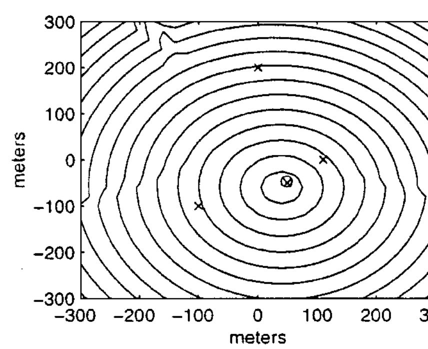

c) $\mu = 10^2$ and $f_\ell(t_0) = [1, 1, .01, 1]$ kg

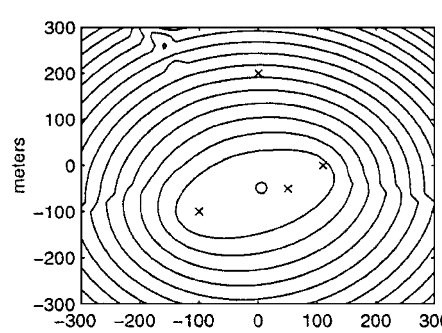

d) $\mu = 10^2$ and $f_\ell(t_0) = [.01, 1, 1, .01]$ kg

Fig. 4 Contour plots of the function J.

Define $\bar{\mathcal{D}}_j$ as the closure of $\mathcal{D}_j$, that is,

$$\bar{\mathcal{D}}_j = \bigcap_{i \ne j} \left\{\boldsymbol{x} \in \mathbb{R}^3 : \frac{M_j}{\tau_j}\|\boldsymbol{d}_j - \boldsymbol{x}\| \ge \frac{M_i}{\tau_i}\|\boldsymbol{d}_i - \boldsymbol{x}\|\right\}$$

Each pair of spacecraft define the line

$$\left\{\boldsymbol{x} \in \mathbb{R}^3 : (M_j/\tau_j)\|\boldsymbol{d}_j - \boldsymbol{x}\| = (M_i/\tau_i)\|\boldsymbol{d}_i - \boldsymbol{x}\|\right\}$$

These lines form the boundaries of $\mathcal{D}_j$. Figure 5 shows a sequence of plots that describe how $\mathcal{D}_3$ is defined for a constellation of four spacecraft. Figures 5a–5c define the regions corresponding to $(M_3/\tau_3)\|\boldsymbol{d}_3 - \boldsymbol{x}\| > (M_1/\tau_1)\|\boldsymbol{d}_4 - \boldsymbol{x}\|$, $(M_3/\tau_3)\|\boldsymbol{d}_3 - \boldsymbol{x}\| > (M_2/\tau_2)\|\boldsymbol{d}_2 - \boldsymbol{x}\|$, and $(M_3/\tau_3)\|\boldsymbol{d}_3 - \boldsymbol{x}\| > (M_4/\tau_4)\|\boldsymbol{d}_1 - \boldsymbol{x}\|$, respectively. Figure 5d defines the region $\mathcal{D}_3$ as the intersection of these three regions. In a similar manner, regions $\mathcal{D}_1$, $\mathcal{D}_2$, and $\mathcal{D}_4$ can be defined.

The following two lemmas ensure that for any configuration of N spacecraft, there are at most N disjoint regions that completely fill $\mathbb{R}^3$.

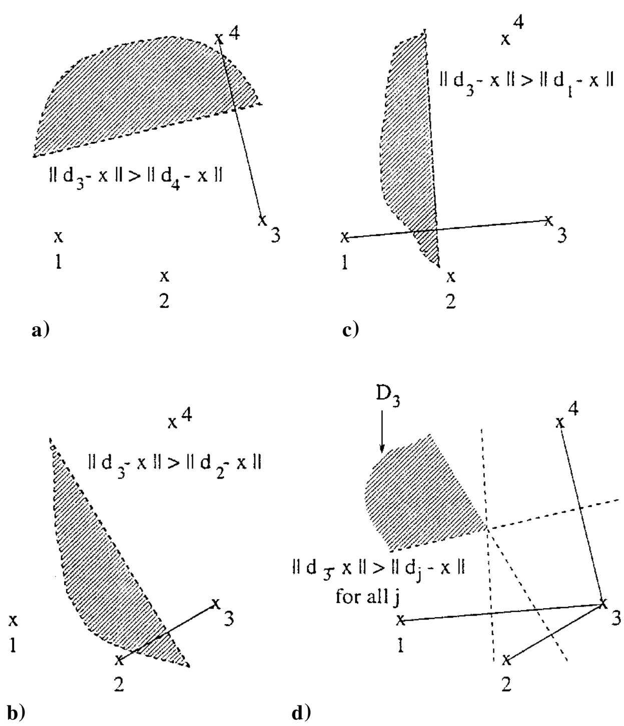

Fig. 5 Defining region $\mathcal{D}_3$ for the objective function J.

Lemma 1: $\mathcal{D}_i \cap \mathcal{D}_j = \emptyset, i \neq j$.

Proof: See the Appendix.

Lemma 2: The $\bigcup_{i=1}^{N} \bar{\mathcal{D}}_i = \mathbb{R}^N$.

Proof: See the Appendix.

The contours in Fig. 4a indicate that although J is not convex, it is continuous and has a unique minimum. The question is whether a gradient descent algorithm can be used to minimize J. The following theorem characterizes the continuity of J and its gradient.

Theorem 1: If

$$\sum_{\ell=1}^{N} f_\ell(t_f) \neq 0$$

then the following statements hold.

1) $J(\boldsymbol{r}_R)$ is continuous on $\mathbb{R}^3$.

2) If $M_i/\tau_i = M_j/\tau_j$ for all $i, j \in 1, \ldots, N$, then $J(\boldsymbol{r}_R)$ is continuously differentiable on $\mathbb{R}^3$.

3) Otherwise, it is continuously differentiable on $\bigcup_{\ell=1}^{N} \mathcal{D}_\ell$ (but not on the boundaries).

Proof: See the Appendix.

Optimization Procedure

All that remains is to choose an optimization algorithm that minimizes J in Eq. (2) to find the fuel optimal center of rotation $\boldsymbol{r}_R$. Because gradient information is available, it is possible to use a gradient descent algorithm that is modified to handle the possible discontinuities between the regions $\mathcal{D}_\ell$. An alternative is to use a direct search method such as the Nelder–Mead Simplex method described in Refs. 15 and 16 (pp. 305–309). The advantage for this particular problem is that derivative information is not used, and the algorithm easily passes over the discontinuities in the gradient. Also, efficient implementations of the Nelder–Mead algorithm exist (Ref. 17, pp. 2.4–2.5). One of the disadvantages of the Nelder–Mead algorithm is that it can be very expensive and/or time consuming for problems with objective functions that are severely elongated or when the dimensions of the problem become large.[15] Because Eq. (2) does not suffer from either of these problems, it appears to be well suited for our application. The Nelder–Mead algorithm is

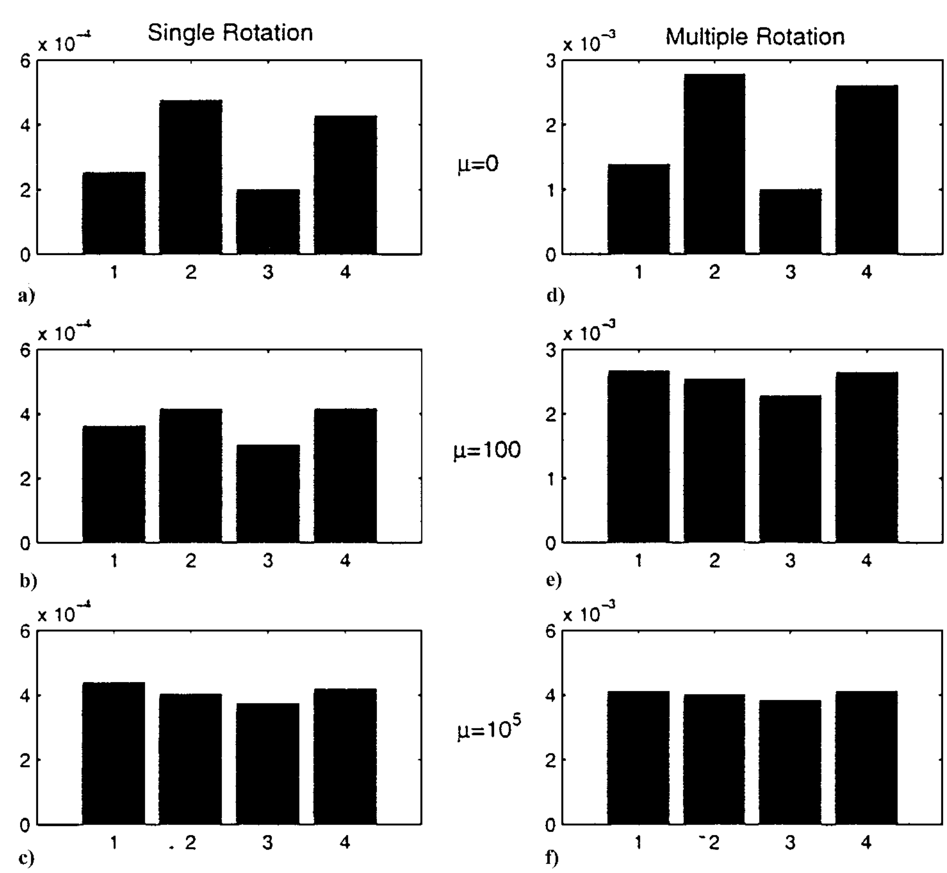

Fig. 6 Fuel used after a single rotation.

initialized, by using the center of inverse fuel mass at time t_0, defined in Eq. (17) and shown with a ○ in Fig. 4. The point $\boldsymbol{r}_R^{(0)}$ is seen to be relatively close to the desired minimum of J.

Based on the constellation rotation trajectory determined by the optimization process, the open-loop control law for each of the ℓ spacecraft can be found:

$$\boldsymbol{T}_\ell = M_\ell \boldsymbol{a}_\ell = M_\ell(\boldsymbol{a}_{r\ell} + \boldsymbol{a}_{t\ell})$$

$$= \begin{cases} M_\ell[\alpha z \times \boldsymbol{r}_{R\ell} + (\alpha t)^2 z \times (z \times \boldsymbol{r}_{R\ell})], & 0 \le t \le t_w \\ M_\ell(\alpha t_w)^2 z \times (z \times \boldsymbol{r}_{R\ell}), & t_w \le t \le t_f - t_w \\ M_\ell[-\alpha z \times \boldsymbol{r}_R \ell + (\alpha(t_f - t))^2 z \\ \quad \times (z \times \boldsymbol{r}_{R\ell})], & t_f - t_w \le t \le t_f \end{cases} \tag{18}$$

The torque for $0 \le t \le t_w$ causes the formation to spin up, the torque for $t_w \le t \le t_f - t_w$ causes the formation to spin at a constant rate, and the torque for $t_f - t_w \le t \le t_f$ causes the formation to spin down.

Simulation Results

This section describes simulation results using the approach described in this paper. Simulations were performed in MATLAB® and Simulink. The numerical values used for the simulation are given in Table 1 with the exception that the mass distribution is changed to $M = (200, 200, 200, 200)$ kg. The initial fuel distribution is $f_\ell(t_0) = (1, 1, 1, 1)$ kg. The parameter μ allows tradeoffs between minimizing the total fuel used and equalizing fuel across the formation. When $\mu = 0$ fuel is minimized, as $\mu \to \infty$ fuel is equalized. The fuel used by each spacecraft after a single 90-deg rotation is shown in Fig. 6. Figure 6a is for $\mu = 0$, that is, fuel minimization; Fig. 6b is for $\mu = 100$, that is, a tradeoff between fuel minimization and fuel equalization; and Fig. 6c is when $\mu = 10^5$, that is, fuel equalization. The total fuel used by all of the spacecraft is 0.0014 kg for $\mu = 0$, 0.0015 kg for $\mu = 100$, and 0.0016 kg for $\mu = 10^5$. Notice that when fuel is equalized, it is not necessarily minimized. In general, minimization and equalization are conflicting criteria.

The fuel used after 15 consecutive randomly selected rotations is also shown in Fig. 6. Cases where $\mu = 0$, $\mu = 100$, and $\mu = 10^5$ are shown in Figs. 6a, 6b, and 6c, respectively. For $\mu = 0$ the total fuel used was 0.0058 kg, for $\mu = 100$ kg the total fuel used was 0.0107 kg, and for $\mu = 10^5$ the total fuel used was 0.0116 kg.

Conclusions

The physical location of the axis about which a constellation of spacecraft rotates determines the fuel consumed by each spacecraft during the maneuver. We have derived an algorithm that finds the optimal location for the axis of rotation, trading off overall fuel minimization and fuel equalization across a constellation of spacecraft in free space. The simulation results show that fuel minimization and fuel equalization are conflicting criteria. Note that minimum fuel rotations will result in fuel starvation for some spacecraft. Fuel is simultaneously minimized and equalized only if the spacecraft are an equal distance from the center of inverse fuel mass, and the thrust capabilities of the spacecraft are identical. This would be the case for three identical spacecraft in an equilateral triangle, but is not true if the spacecraft are not identical.

The control law derived defines fuel optimal trajectories for each spacecraft in the constellation. These trajectories could be used for feedforward control, with additional feedback used for robustness to uncertainties and disturbance rejection. Because the approach taken is conservative (only the most performance-limited spacecraft is at its thrust limit at just two instants during the trajectory), the additional thrust required for feedback control could be easily accommodated by the spacecraft implying that the prescribed trajectories would still be feasible.

Finally, the optimization algorithm described could be used to determine the amount of fuel required by an entire interferometry mission. If the desired life of the mission and the desired star locations are known, the amount of fuel required to transition between stars can be estimated with the algorithm described. This could be embedded in a larger optimization algorithm that computes the optimal sequence of stars and the resulting fuel required for each spacecraft. If it is desired, for cost purposes, that the spacecraft be identical, then the optimization algorithm should be performed with large μ.

Appendix: Proofs

Proof of Lemma 1

Suppose that $x \in \mathcal{D}_i \cap \mathcal{D}_j$, then

$$x \in \mathcal{D}_i \Rightarrow (M_i/\tau_i)\|\boldsymbol{d}_i - \boldsymbol{x}\| > (M_j/\tau_j)\|\boldsymbol{d}_j - \boldsymbol{x}\|$$

$$x \in \mathcal{D}_j \Rightarrow (M_j/\tau_j)\|\boldsymbol{d}_j - \boldsymbol{x}\| > (M_i/\tau_i)\|\boldsymbol{d}_i - \boldsymbol{x}\|$$

which is a contradiction.

Proof of Lemma 2

Pick an arbitrary $\boldsymbol{x} \in \mathbb{R}^3$. Suppose that $\boldsymbol{x} \notin \bigcup_{i=1}^N \bar{\mathcal{D}}_i$. Now $\boldsymbol{x} \notin \bar{\mathcal{D}}_1 \Rightarrow (M_1/\tau_1)\|\boldsymbol{d}_1 - \boldsymbol{x}\| < (M_{\hat{j}}/\tau_{\hat{j}})\|\boldsymbol{d}_{\hat{j}} - \boldsymbol{x}\|$ for some $\hat{j} \in \{2, \ldots, N\}$. Renumber the spacecraft such that $\hat{j} = 2$, then $(M_1/\tau_1)\|\boldsymbol{d}_1 - \boldsymbol{x}\| < (M_2/\tau_2)\|\boldsymbol{d}_2 - \boldsymbol{x}\|$. Now $\boldsymbol{x} \notin \bar{\mathcal{D}}_2 \Rightarrow (M_2/\tau_2)\|\boldsymbol{d}_2 - \boldsymbol{x}\| < (M_{\hat{j}}/\tau_{\hat{j}})\|\boldsymbol{d}_{\hat{j}} - \boldsymbol{x}\|$ for some $\hat{j} \in \{3, \ldots, N\}$. Renumber the spacecraft such that $\hat{j} = 3$, then $(M_1/\tau_1)\|\boldsymbol{d}_1 - \boldsymbol{x}\| < (M_2/\tau_2)\|\boldsymbol{d}_2 - \boldsymbol{x}\| < (M_3/\tau_3)\|\boldsymbol{d}_3 - \boldsymbol{x}\|$. Repeat the argument for $\bar{\mathcal{D}}_3, \ldots, \bar{\mathcal{D}}_{N-1}$ to get

$$(M_1/\tau_1)\|\boldsymbol{d}_1 - \boldsymbol{x}\| < (M_2/\tau_2)\|\boldsymbol{d}_2 - \boldsymbol{x}\| < \cdots < (M_N/\tau_N)\|\boldsymbol{d}_N - \boldsymbol{x}\|$$

Now $\boldsymbol{x} \notin \bar{\mathcal{D}}_N \Rightarrow (M_N/\tau_N)\|\boldsymbol{d}_N - \boldsymbol{x}\| < (M_{\hat{j}}/\tau_{\hat{j}})\|\boldsymbol{d}_{\hat{j}} - \boldsymbol{x}\|$ for some $\hat{j} \in \{1, \ldots, N-1\}$, which is a contradiction.

Proof of Theorem 1

Differentiating Eq. (2) with respect to $\boldsymbol{r}_R$ gives

$$\frac{\partial J}{\partial \boldsymbol{r}_R} = \sum_{\ell=1}^N -2[f_\ell(t_0) - f_\ell(t_f)]\frac{\partial f_\ell(t_f)}{\partial \boldsymbol{r}_R}$$
$$+ \sum_{\ell=1}^N \log\left[\frac{f_\ell(t_f)}{\Sigma_j f_j(t_f)}\right]\left(\left\{\left[\sum_j f_j(t_f)\right]\frac{\partial f_\ell(t_f)}{\partial \boldsymbol{r}_R}\right.\right.$$
$$\left.\left. - f_\ell(t_f)\left[\sum_j \frac{\partial f_j(t_f)}{\partial \boldsymbol{r}_R}\right]\right\}\Big/\left[\sum_j f_j(t_f)\right]^2\right)$$

Assuming that

$$\sum_j f_j(t_f) > 0$$

then $\partial J/\partial \boldsymbol{r}_R$ is continuous if $f_i(t_f)$ and $\partial f_i(t_f)/\partial \boldsymbol{r}_R$ are continuous in $\boldsymbol{r}_R$. From Eqs. (16), (9), and (11), we obtain the following expression for $f_i(t_f)$:

$$f_i(t_f) = f_i(t_0)$$
$$- \gamma M_i \|\boldsymbol{d}_i\|\left[\frac{2\hat{\phi}}{t_f(1-c)} + \frac{\hat{\phi}^2}{t_f(1-c)^2} - \frac{4\hat{\phi}^2 c}{3t_f(1-c)^2}\right]$$

Both c and $\|\boldsymbol{d}_i\|$ depend on $\boldsymbol{r}_R$ so that

$$\frac{\partial f_i(t_f)}{\partial \boldsymbol{r}_R} = \frac{\partial f_i(t_f)}{\partial \|\boldsymbol{d}_i\|}\frac{\partial \|\boldsymbol{d}_i\|}{\partial \boldsymbol{r}_R} + \frac{\partial f_i(t_f)}{\partial c}\frac{\partial c}{\partial \boldsymbol{r}_R}$$

where

$$\frac{\partial f_i(t_f)}{\partial \|\boldsymbol{d}_i\|} = -\gamma M_i\left[\frac{2\hat{\phi}}{t_f(1-c)} + \frac{\hat{\phi}^2}{t_f(1-c)^2} - \frac{4\hat{\phi}^2 c}{t_f(1-c)^2}\right]$$

is a continuous function of $\|\boldsymbol{d}_i\|$ and

$$\frac{\partial f_i(t_f)}{\partial c} = -\gamma M_i\left[\frac{2\hat{\phi}}{t_f(1-c)^2} + \frac{2\hat{\phi}^2}{t_f(1-c)^3} - \frac{4\hat{\phi}^2(1+c)}{t_f(1-c)^3}\right]$$

is continuous in c as long as $c \in [0, \frac{1}{2}]$. Here $\|\boldsymbol{d}_i\| = \|(I - zz^T)(\boldsymbol{r}_i - \boldsymbol{r}_R)\|$ is clearly a continuously differentiable function of $\boldsymbol{r}_R$, and so the continuity properties of J are determined by the continuity properties of c, where c is a root of the sixth-order polynomial given in Eq. (12), which can be rewritten in the following form that is standard for the Evans root locus:

$$1 + \frac{1}{K}\left[\frac{-(\hat{\phi}^4 + \hat{\phi}^2)c^2 + 2\hat{\phi}^2 c - \hat{\phi}^2}{c^6 - 4c^5 + 6c^4 - 4c^3 + c^2}\right] = 0$$

By standard root locus theory, the roots are a continuous function of $1/K = \|\boldsymbol{d}_\beta\|^2 M_\beta^2/\tau_\beta^2 t_f^4$, where $\|\boldsymbol{d}_\beta\|$ and β are functions of $\boldsymbol{r}_R$. Here β is a constant function of $\boldsymbol{r}_R$ in each region $\mathcal{D}_j$, with a discontinuous switch on the boundaries. Therefore, $1/K$ will also be a continuous function of $\boldsymbol{r}_R$ on each region, thereby establishing statement 3 of the lemma. At the boundaries $\|\boldsymbol{d}_\beta\|$ is continuous (but not differentiable) and so $1/K$ is continuous at the boundary if $M_i/\tau_i = M_j/\tau_j$ for all i and j, establishing statement 2. Because $\partial J/\partial \boldsymbol{r}_R$ is continuous for all but a set of measure zero (the region boundaries), J is continuous on all of $\mathbb{R}^3$.

Acknowledgments

This work was performed in part at the Jet Propulsion Laboratory, California Institute of Technology under contract with NASA. The research at Brigham Young University was supported by the Jet Propulsion Laboratory, California Institute of Technology under Contract 96-1245. The authors thank the reviewers for their helpful comments.

References

[1]Lau, K., Lichten, S., Young, L., and Haines, B., "An Innovative Deep Space Application of GPS Technology for Formation Flying Spacecraft," *AIAA Guidance, Navigation, and Control Conference*, AIAA, Reston, VA, 1996, pp. 96–381.

[2]Cover, T. M., and Thomas, J. A., *Elements of Information Theory*, Wiley, New York, 1991, pp. 12–15.

[3]Wang, P. K. C., and Hadaegh, F. Y., "Coordination and Control of Multiple Microspacecraft Moving in Formation," *Journal of Astronautical Sciences*, Vol. 44, No. 3, 1996, pp. 315–355.

[4]Wang, P., Hadaegh, F., and Lau, K., "Synchronized Formation Rotation and Attitude Control of Multiple Free-Flying Spacecraft," *Journal of Guidance, Control, and Dynamics*, Vol. 22, No. 1, 1999, pp. 28–35.

[5]DeCou, A. B., "Orbital Station-Keeping for Multiple Spacecraft Interferometry," *Journal of Astronautical Sciences*, Vol. 39, July–Sept. 1991, pp. 283–297.

[6]McInnes, C. R., "Autonomous Ring Formation for a Planar Constellation of Satellites," *Journal of Guidance, Control, and Dynamics*, Vol. 18, No. 5, 1995, pp. 1215–1217.

[7]Ulybyshev, Y., "Long-Term Formation Keeping of Satellite Constellation Using Linear-Quadratic Controller," *Journal of Guidance, Control, and Dynamics*, Vol. 21, No. 1, 1998, pp. 109–115.

[8]Beard, R., Frost, R., and Stirling, W., "A Hierarchical Coordination Scheme for Satellite Formation Initialization," *AIAA Guidance, Navigation, and Control Conference*, AIAA, Reston, VA, 1998, pp. 677–685.

[9]Beard, R., "Architecture and Algorithms for Constellation Control," TR, Jet Propulsion Lab., California Inst. of Technology, Pasadena, CA, March 1998.

[10]Beard, R. W., and Hadaegh, F. Y., "Constellation Templates: An Approach to Autonomous Formation Flying," *World Automation Congress*, ISIAC, 1998, pp. 177.7–177.6.

[11]Beard, R. W., McLain, T. W., and Hadaegh, F. Y., "Fuel Equalized Retargeting for Separated Spacecraft Interferometry," *American Control Conference*, 1998, pp. 1580–1584.

[12]Beard, R. W., and Hadaegh, F. Y., "Fuel Optimized Rotation for Satellite Formations in Free Space," *American Control Conference*, 1999, pp. 2975–2979.

[13]Wertz, J. R. (ed.), *Spacecraft Attitude Determination and Control*, Kluwer Academic, Norwell, MA, 1978.

[14]Athans, M., and Falb, P., *Optimal Control*, McGraw–Hill, New York, 1966, pp. 675–710.

[15]Wright, M. H., "Direct Search Methods: Once Scorned, Now Respectable," *Numerical Analysis*, edited by D. F. Griffiths and G. A. Watson, Pitman Research Notes in Mathematics, Addison Wesley Longman, Reading, MA, 1995, pp. 191–208.

[16]Press, W. H., Flannery, B. P., Teukolsky, S. A., and Vetterling, W. T., *Numerical Recipes in C: The Art of Scientific Computing*, Cambridge Univ. Press, New York, 1988, pp. 305–309.

[17]"MATLAB Optimization Toolbox," MathWorks, Natick, MA, 1994, pp. 2.4–2.5.